was carried out according to standard procedures[24d] using as a reference spectrum that of the [Fe^{II}DMF] complex. The spectral characteristics of the [Fe^{II}DMF] and [$Fe^{II}Cl]^-$ complexes in the Soret region are given in Table II. The molecular extinction coefficients of the two complexes at their respective maximum of absorption exhibit usual values ((2–4) $\times 10^5$ M^{-1} cm^{-1}).

Acknowledgment. This work was supported in part by the CNRS (Equipe de Recherche Associée 309 "Electrochimie Moléculaire").

Registry No. DMF, 68-12-2; Fe^{III}(TAP)Cl, 90837-94-8; Fe^{III}(e-$(C12)_2$-AC)Cl, 90837-95-9; Fe^{III}(e$(C12)_2$-AT)Cl, 90898-37-6; Fe^{III}(e-$(C12)_2$-CT)Cl, 79198-03-1; Fe^{III}(e[di(C4)Ph]$_2$-CT)Cl, 83460-51-9; $[Fe^{III}(TAP)Cl]^-$, 90837-96-0; $[Fe^{II}(e(C12)_2\text{-}AC)Cl]^-$, 90837-97-1; $[Fe^{II}(e(C12)_2\text{-}AT)Cl]^-$, 90898-38-7; $[Fe^{II}(e(C12)_2\text{-}CT)Cl]^-$, 90837-98-2; $[Fe^{II}(e[di(C4)Ph]_2\text{-}CT)Cl]^-$, 90837-99-3; $[Fe^{I}(TAP)]^-$, 90838-00-9; $[Fe^{I}(e(C12)_2\text{-}AC)]^-$, 90838-01-0; $[Fe^{I}(e(C12)_2\text{-}AT)]^-$, 90838-02-1; $[Fe^{I}(e(C12)_2\text{-}CT)]^-$, 79209-91-9; $[Fe^{I}(e[di(C4)Ph]_2\text{-}CT)]^-$, 90838-03-2; $[Fe^{I}\cdot(TAP)]^{2-}$, 90838-04-3; $[Fe^{I}\cdot(e(C12)_2\text{-}AC)]^{2-}$, 90838-05-4; $[Fe^{I}\cdot(e(C12)_2\text{-}AT)]^{2-}$, 90898-39-8; $[Fe^{I}\cdot(e(C12)_2\text{-}CT)]^{2-}$, 90838-06-5; $[Fe^{I}\cdot(e[di(C4)Ph]_2\text{-}CT)]^{2-}$, 90838-07-6; Fe^{II}(DMF)(TAP), 90838-08-7; Fe^{II}(DMF)(e$(C12)_2$-AC), 90838-09-8; Fe^{II}(DMF)(e$(C12)_2$-AT), 90898-40-1; Fe^{II}(DMF)(e$(C12)_2$-CT), 90838-10-1; Fe^{II}(DMF)(e[di(C4)-Ph]$_2$-CT), 90838-11-2; Fe^{III}(TPP)Cl, 16456-81-8; Fe^{III}(a$(C12)_2$-CT)Cl, 90838-12-3; Fe^{III}(a$(C12)_2$-AT)Cl, 90838-13-4; Fe^{III}(a$(C12)_2$-AC)Cl, 90898-41-2; Fe^{III}(aPF)Cl, 86107-94-0; $[Fe^{II}(TPP)Cl]^-$, 84537-58-6; $[Fe^{II}(a(C12)_2\text{-}CT)Cl]^-$, 90838-14-5; $[Fe^{II}(a(C12)_2\text{-}AT)Cl]^-$, 90838-15-6; $[Fe^{II}(a(C12)_2\text{-}AC)Cl]^-$, 90898-42-3; $[Fe^{II}(aPF)Cl]^-$, 86124-06-3; Fe^{II}-(DMF)(TPP), 90838-16-7; Fe^{II}(DMF)(a$(C12)_2$-CT), 90838-17-8; Fe^{II}(DMF)(a$(C12)_2$-AT), 90838-18-9; Fe^{II}(DMF)(a$(C12)_2$-AC), 90898-43-4; Fe^{II}(DMF)(aPF), 90838-19-0; $[Fe^{I}(TPP)]^-$, 54547-68-1; $[Fe^{I}(a(C12)_2\text{-}CT)]^-$, 90838-20-3; $[Fe^{I}(a(C12)_2\text{-}AT)]^-$, 90838-21-4; $[Fe^{I}(a(C12)_2\text{-}AC)]^-$, 90898-44-5; $[Fe^{I}(aPF)]^-$, 90857-60-6; $[Fe^{I}\cdot(TPP)]^{2-}$, 90838-22-5; $[Fe^{I}\cdot(a(C12)_2\text{-}CT)]^{2-}$, 90838-23-6; $[Fe^{I}\cdot(a-(C12)_2\text{-}AT)]^{2-}$, 90838-24-7; $[Fe^{I}\cdot(a(C12)_2\text{-}AC)]^{2-}$, 90898-45-6; $[Fe^{I}\cdot(aPF)]^{2-}$, 90838-25-8; $LiClO_4$, 7791-03-9; NBu_4BF_4, 429-42-5; chlorine, 7782-50-5.

Hemocyanin Models: Synthesis, Structure, and Magnetic Properties of a Binucleating Copper(II) System

Vickie McKee, Maruta Zvagulis, Jeffrey V. Dagdigian, Marianne G. Patch, and Christopher A. Reed*

Contribution from the Department of Chemistry, University of Southern California, Los Angeles, California 90089. *Received December 29, 1983*

Abstract: A model compound approach to oxidized hemocyanin is described. The essential structural features of diamagnetism, 3.6-Å copper–copper separation, approximate tetragonal stereochemistry, imidazole ligation, and bridging groups are reproduced in the azide complex $[Cu_2(L\text{-}Et)(N_3)][BF_4]_2$. HL-Et is the septadentate binucleating ligand *N,N,N',N'*-tetrakis(2-(1-ethylbenzimidazolyl))-2-hydroxy-1,3-diaminopropane prepared in good yield via condensation of 1,2-diaminobenzene with 2-hydroxy-1,3-diaminopropanetetraacetic acid. Related complexes $[Cu_2(L\text{-}Et)X]^{2+}$ where X^- = OAc^-, $HCOO^-$, NO_2^-, and pyrazolate have quite different magnetic properties. The acetate is ferromagnetic ($J \simeq +12$ cm^{-1}) while the nitrite is antiferromagnetic ($J = -139$ cm^{-1}). Crystal structures of the weakly coupled acetate complex $[Cu_2(L\text{-}Et)(OAc)][ClO_4]_2$ (monoclinic, $P2_1/n$, $a = 14.190$ (3) Å, $b = 22.707$ (4) Å, $c = 15.883$ (4) Å, $\beta = 97.20$ (2)°, $Z = 4$) and the diamagnetic azide complex $[Cu_2(L\text{-}Et)(N_3)][BF_4]_2$ (monoclinic, $C2/m$, $a = 19.082$ (3) Å, $b = 23.896$ (3) Å, $c = 13.230$ (2) Å, $\beta = 116.21$ (1)°, $Z = 4$) suggest that these differences have their origin in the orientation of the σ magnetic orbitals with respect to the bridging ligands. The particular mode of 1,3-bridging azide in $[Cu_2(L\text{-}Et)(N_3)]^{2+}$, where it is supported by an alkoxide bridge from L-Et, has not been previously observed. It allows close approach of the copper(II) atoms (3.615 (3) Å) and thus becomes a viable stereochemistry for metazidohemocyanin. The present studies support the idea that tetragonality of the copper(II) stereochemistry is important for attaining diamagnetism in oxy- and methemocyanins and that alkoxide from serine or threonine would be well suited to the role of a bridging endogenous ligand.

A long-standing problem in bioinorganic chemistry is understanding how hemocyanin[1] functions as an oxygen carrier. The operative states of this dinuclear copper protein are the colorless Cu(I) deoxy form, Hc, and the blue Cu(II) oxy form, HcO_2. Their structures are modestly well-defined by a recent accumulation of chemical and spectroscopic data such that Scheme I, with some caveats, can be adopted as a working model.

For the deoxy state, the essential spectroscopic invisibility of Cu(I) leaves mainly EXAFS studies[2,3] and its reactivity with carbon monoxide[4] as a guide to structure. While the precise coordination number and stereochemistry are unknown, it is known that there are at least two histidines per copper and some form

Scheme I. Possible Structures for Various States of Hemocyanin[a]

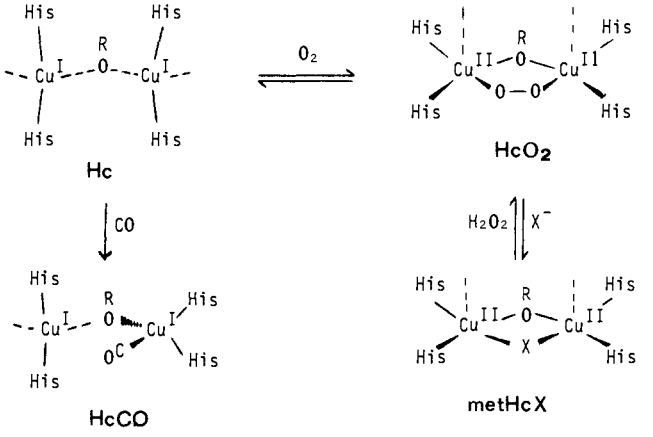

[a] Dashed lines are used to indicate uncertainty in coordination number.

(1) For reviews on hemocyanin see: (a) van Holde, K. E.; Miller, K. I. *Q. Rev. Biophys.* **1982**, *15*, 1–129. (b) Lontie, R.; Witters, In "Inorganic Biochemistry"; Eichhorn, G. L., Ed.; Elsevier: New York, 1973; Vol. 1, Chapter 12; (c) Lontie, R.; Vanquickenborne, L. In "Metal Ions in Biological Systems" Siegel, H., Ed.; Marcel Dekker: New York, 1974; Vol. 3, pp 183–200. (d) Senozan, N. M. *J. Chem. Educ.* **1976**, *53*, 684–688. (e) Solomon, E. I. In "Metal Ions in Biology"; Spiro, T. G., Ed.; Wiley-Interscience: New York, 1981; Vol. 3, pp 41–108. (f) Bonaventura, J.; Bonaventura, C. *Am. Zool.* **1980**, *20*, 7–17. (g) Owen, C. A. "Biochemical Aspects of Copper"; Noyes: New Jersey, 1982; pp 41–48.

(2) (a) Brown, J. M.; Powers, L.; Kincaid, B.; Larrabee, J. A.; Spiro, T. G. *J. Am. Chem. Soc.* **1980**, *102*, 4210–4216. (b) Woolery, G. L.; Powers, L.; Winkler, M.; Solomon, E. I.; Spiro, T. G. *Ibid.* **1984**, *106*, 86–92.

(3) Co, M. S.; Scott, R. A.; Hodgson, K. O. *J. Am. Chem. Soc.* **1981**, *103*, 986–988.

0002-7863/84/1506-4765$01.50/0

of stoichiometric control that allows binding of only one CO per dicopper(I) site in HcCO. An appealing proposal to account for this is based on the observation that CO binding occurs much more readily to *three*-coordinate copper(I) than to *two*-coordinate copper(I).[5] Also from model compounds, bis(imidazole) ligation about copper(I) seems to show a predilection for an approximately linear orientation.[6,7] RO^- is a possible endogenous bridging ligand for copper(I) whose presence, or that of a different third ligand, would rationalize the longer average Cu–N bond length (1.95 (2) Å) in Hc compared to cationic bis(imidazole)copper(I) complexes (1.87–1.92 Å).[7] Thus, the indicated structures for Hc and HcCO in Scheme I are reasonable, but by no means exclusive, representations of the copper(I) coordination chemistry.

Dioxygen binding involves dinuclear copper(II) chemistry. Resonance Raman studies[8] indicate symmetrically bridging peroxide ($\nu(O_2) \simeq 745$ cm^{-1}) and the collective evidence from magnetic,[9] chemical, and electronic data[10] suggests the structure for HcO_2 shown in Scheme I. Diamagnetism, approximate tetragonal stereochemistry and an endogenous protein bridging ligand, RO^-, are key features of the proposed structure. Displacement of peroxide by various anions $X^- = N_3^-$, OAc^-, Cl^-, NCS^-, etc. leads to exogenous-bridged methemocyanin derivatives, metHcX, whose physical properties closely parallel those of HcO_2.

The foregoing structural picture of the active site of hemocyanin has sufficient definition to warrant a detailed model compound approach. Our starting point in this endeavor has been to develop synthetic models for methemocyanin derivatives. These were chosen because, to be useful, they must fit relatively exacting criteria. Moreover, the close structural and spectroscopic similarity of methemocyanin derivatives to oxyhemocyanin makes them particularly relevant to gaining an understanding of how to solve the more challenging problem of reversible oxygen binding. Reaction models for reversible oxygen binding have been reported,[11] but, so far, they have resisted definitive structural characterization.

At question in copper(II) forms of hemocyanin, as well as in other type III binuclear copper protiens such as tyrosinase,[1e] is the identity of the bridging ligand(s), the origin of the diamagnetism, and the precise definition of the copper coordination chemistry. Phenoxide from tyrosine is a popular choice for an endogenous bridging ligand. Such an anionic O atom donor is consistent with the assignment of the 425-nm UV–vis absorption of HcO_2 to phenoxide → Cu(II) charge transfer,[10] but the expected enhancement of tyrosinate vibrational modes in resonance Raman studies is not seen, at least by using the reported excitation wavelengths.[8] The absence of distinct absorptions in the 400–500-nm region for a thiourea-treated HcO_2 has been interpreted as evidence against tyrosinate coordination.[12] While the specific identity of the bridging ligand is uncertain, a phenoxide-like ligand remains the most likely possibility because of the widely demonstrated ability of anionic O-atom bridges to act as superior mediators of antiferromagnetic coupling.[13] EXAFS data are not compatible with a heavier donor atom,[14] and suitable N atom bridges are not easily envisaged. Approximate tetragonal stereochemistry about copper has been inferred from electronic spectroscopy,[10] but the coordination number is uncertain. Overall four- or five-coordination is most likely with two[14] or three[2] additional N or O atom donors, two of which must be imidazole from histidine.[14] The Cu···Cu separation is close to 3.6 Å[2,14] in HcO_2 and is 3.66 Å in metHc(N_3).[2b]

In this paper we amplify upon our initial communication[15] which indicated that the defined structural chemistry of copper(II) hemocyanin derivatives can be replicated in an appropriately chosen model compound. The results set limits upon the coordination requirements of the dicopper(II) active site in metHcX and HcO_2, and they offer a rationale for their diamagnetism. They also suggest that alkoxide is well suited to act as an endogenous bridging ligand. An unusual mode of azide bridging is observed in the model compound, and this raises the question of 1,1- vs. 1,3-azide bridging in metHc(N_3).

Experimental Section

Synthesis. All materials were A.R. grade and used without purification except for tetrahydrofuran that was dried by distillation from sodium/benzophenone inside an inert-atmosphere glovebox. Caution! While none of the present perchlorate complexes has proved to be shock sensitive, care is recommended. All new reactions were done on a 50–100-mg scale, and no quantities larger than 300 mg were isolated at any one time.

***N,N,N',N'*-Tetrakis(2-(1-ethylbenzimidazolyl))-2-hydroxy-1,3-diaminopropane, HL-Et.** 1,2-Diaminobenzene (10.55 g, 0.097 mol) was ground to a fine powder and intimately mixed with 2-hydroxy-1,3-diaminopropanetetraacetic acid (5.0 g, 0.016 mol). The mixture was heated at 170–180 °C for 1 h at which stage effervescence had ceased. After the mixture was cooled, the resulting red glass was taken up in dilute (~4 M) hydrochloric acid (~150 mL), and a grayish blue precipitate was slowly formed. After the solution was filtered, this precipitate was washed by slurrying in acetone several times. The precipitate was then dissolved in water and neutralized with dilute ammonia. The off-white precipitate was collected, recrystallized from acetone, and ground to a fine powder prior to vacuum drying (5 g, 90%). After being thoroughly dried, this material was suspended in dry tetrahydrofuran (50 mL) and stirred overnight with NaOH (1.4 g). Bromoethane (9 g) was added, and the solution was left stirring for 2 days. The solvents were then stripped to dryness and the resulting powder dissolved in chloroform. The insoluble NaBr was removed by filtration, and the filtrate was stripped to a very small volume. A little acetone was added, and upon standing a white powder was deposited (4.46 g, 83%). After the precipitate was vacuum dried, elemental analysis and ^{1}H NMR were consistent with a hemihydrate: ^{1}H NMR ($CDCl_3$) δ 1.1 (3, 3 H), 2.7 (2, 1 H), 3.95 (4, 2 H), 4.0 (1, 2 H), 7.4 (m, 4 H). Anal. Calcd for $C_{43}N_{10}H_{51}O_{1.5}$: C, 70.56; H, 7.02; N, 19.14. Found: C, 70.58; H, 6.86; N, 18.94. The analogous propyl ligand HL-Pr was preparated by a similar procedure and characterized by ^{1}H NMR ($CDCl_3$): δ 0.7 (3, 3 H), 1.5 (4, 2 H), 2.7 (3, 2 H), 4.0 (4, 2 H), 7.1–7.6 (m, 4 H).

$[Cu_2(HL\text{-}Et)(H_2O)_4][ClO_4]_4H_2O$. Ethanolic solutions of $Cu(ClO_4)_2 \cdot 6H_2O$ (0.31 g) and HL-Et (0.3 g) were mixed, and the resulting blue precipitate was collected. A sample for analysis was recrystallized from acetonitrile–ether by vapor diffusion. Anal. Calcd for $C_{43}H_{60}N_{10}Cl_4O_{22}Cu_2$: C, 38.60; H, 4.52; N, 10.47. Found: C, 38.63; H, 4.25; N, 10.45.

$[Cu_2(HL\text{-}Et)(H_2O)_4][BF_4]_4 \cdot H_2O$: prepared as above using $Cu(BF_4)_2 \cdot 6H_2O$. Anal. Calcd for $C_{43}H_{60}N_{10}F_{16}B_4O_6Cu_2$: C, 42.0; H, 4.9; N, 10.0. Found: C, 41.8; H, 4.6; N, 10.5.

$[Cu_2(L\text{-}Et)X][Y]_2 \cdot nH_2O$ for $X^- = OAc^-$, $HCOO^-$, N_3^-, NO_2^-, and Pyrazolate (pyl) and $Y^- = BF_4^-$ and ClO_4^-. Appropriate amounts of NaX salts (1 equiv) were added to ethanol (95%) suspensions of $Cu_2(HL\text{-}Et)(H_2O)_5Y_4$ as prepared above and the mixtures stirred overnight. The products were collected as blue or green hydrates and recrystallized once from acetonitrile–ether by vapor diffusion. Characterizing data are

(4) (a) Vanneste, W.; Mason, H. S. In: "The Biochemistry of Copper"; Peisach, J., Aisen, P., Blumberg, W. E., Eds.; Academic Press: New York, 1966; pp 465–473. (b) Frajer, L. Y.; Alben, J. O. *Biochemistry* **1972**, *11*, 4786–4792.

(5) Sorrell, T. N.; Jameson, D. L. *J. Am. Chem. Soc.* **1982**, *104*, 2053–2054.

(6) Hendriks, H. M. J.; Birker, P. J. M. W. L.; van Rijn, J.; Verschoor, G. C.; Reedijk, J. *J. Am. Chem. Soc.* **1982**, *104*, 3607–3617 and references therein.

(7) Dagdigian, J. V.; McKee, V.; Reed, C. A. *Inorg. Chem.* **1982**, *21*, 1332–1342.

(8) (a) Freedman, T. B.; Loehr, J. S.; Loehr, T. M. *J. Am. Chem. Soc.* **1976**, *98*, 2809–2815. (b) Larrabee, J. A.; Spiro, T. G. *Ibid.* **1980**, *102*, 4217–4223.

(9) Dooley, D. M.; Scott, R. A.; Ellinghaus, J.; Solomon, E. I.; Gray, H. B. *Proc. Natl. Acad. Sci. U.S.A.* **1978**, *75*, 3019–3022.

(10) Solomon, E. I.; Penfield, K. W.; Wilcox, D. E. *Struct. Bond.* **1983**, *53*, 1–57.

(11) (a) Simmons, M. G.; Merrill, C. L.; Wilson, L. J.; Bottomley, L. A.; Kadish, K. M. *J. Chem. Soc., Dalton Trans.* **1980**, 1827. (b) Nishida, Y.; Takahashi, K.; Kuramoto, H.; Kida, S. *Inorg. Chim. Acta* **1981**, *54*, L103–L104.

(12) Kino, J.; Suzuki, S.; Mori, W.; Nakahara, A. *Inorg. Chim. Acta* **1981**, *56*, L33–L34.

(13) (a) Hodgson, D. J. *Prog. Inorg. Chem.* **1975**, *19*, 173–241. (b) Melnik, M. *Coord. Chem. Rev.* **1982**, *42*, 259–293.

(14) Co, M. S.; Hodgson, K. O.; Eccles, T. K.; Lontie, R. *J. Am. Chem. Soc.* **1981**, *103*, 984–986.

(15) McKee, V.; Dagdigian, J. V.; Bau, R.; Reed, C. A. *J. Am. Chem. Soc.* **1981**, *103*, 7000–7001.

Table I. Characterization of Copper(II) Complexes of Type $[Cu_2(L\text{-}Et)(X)]Y_2$

complex	μ_{eff}^{300K}, μ_B/Cu	anal. found (calcd) C	H	N	λ_{max}, mm (ϵ) CH_3CN Nujol			
$[Cu_2(L\text{-}Et)(OAc)][ClO_4]_2$	1.89[a]	46.9 (48.8)	4.6 (4.7)	12.2 (12.65)	800 (sh) 750	1055 (91) 975		
$[Cu_2(L\text{-}Et)(N_3)][ClO_4]_2\cdot H_2O$	diamag	46.8 (46.6)	4.5 (4.5)	16.5 (16.4)	364 (2520) 370	415 (sh) 425 (sh)	705 (201) 710	975 (149) 950
$[Cu_2(L\text{-}Et)(N_3)][BF_4]_2$	diamag[a]	48.8 (48.5)	4.8 (4.6)	16.6 (17.1)	365 (2380) 368	415 (sh) 420	700 (197) 725	980 (140)
$[Cu_2(L\text{-}Et)(pyl)][ClO_4]_2\cdot H_2O$	1.90	48.7 (48.8)	4.7 (4.8)	14.6 (14.8)	710 (sh) 690 (sh)	975 (170) 900		
$[Cu_2(L\text{-}Et)(NO_2)][ClO_4]_2\cdot H_2O$	1.48[a]	46.5 (46.4)	4.42 (4.62)	13.9 (13.6)	745 (91) 745	990 (98) 950 (sh)		
$[Cu_2(L\text{-}Et)(HCOO)][ClO_4]_2\cdot H_2O$	1.83	48.0 (47.6)	4.7 (4.7)	12.7 (12.6)	800 (sh) 750	1060 (106) 975		

[a] See text for more detail.

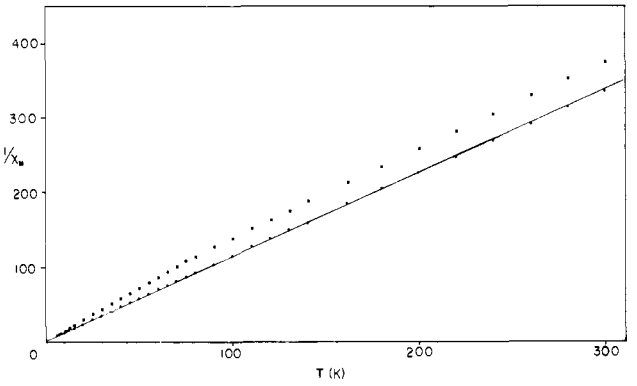

Figure 1. Curie plot for $[Cu_2(HL\text{-}Et)(H_2O)_4][ClO_4]_4\cdot H_2O$ in air (■) and under dry conditions (●). The solid line is a least-squares fit to linearity of the (●) data.

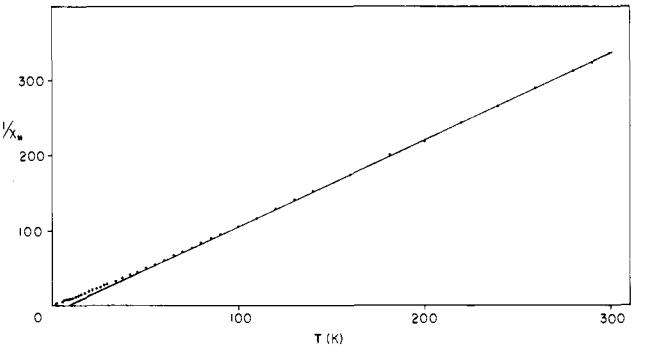

Figure 2. Curie plot for $[Cu_2(L\text{-}Et)(OAc)][ClO_4]_2$. The solid lines is a least-squares fit to linearity of the 70–300 K data.

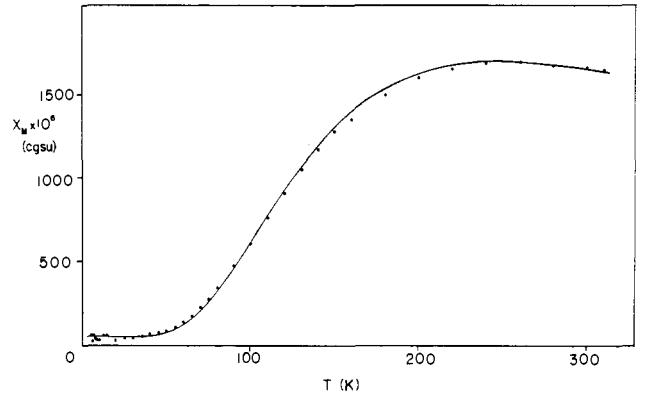

Figure 3. Corrected χ_M data $[Cu_2(L\text{-}Et)(NO_2)][ClO_4]_2\cdot H_2O$. The solid line is a theoretical fit with $J = -139$ cm^{-1}.

shown in Table I. Our preparations of the azide complex showed IR spectra with doublet character to $\nu_{asym}(N_3)$ at 2020 and 2050 cm^{-1} in KBr or Nujol and at 2037 and 2057 cm^{-1} in CH_3CN. Since the molecular structure dictates a single IR-active asymmetric stretching mode, we assign the high-energy, lower intensity band to an impurity. Also, magnetically detectable impurities were found in susceptibility measurements on most samples. Further recrystallization, however, failed to improve product purity.

Magnetic Measurements

Magnetic data were originally collected on a Faraday system at Bell Laboratories by Drs. Frank DiSalvo and Joseph Waszczak. Subsequently, they were collected by using purer samples on an S.H.E. 905 Squid susceptometer at the University of Southern California. Typically, 20–30 mg of finely ground crystalline material was used. Grinding and packing into snap-cap aluminum buckets was done inside a drybox when necessary to avoid hydration problems.

The diamagnetic correction, χ_0, for each complex was estimated by combining the experimentally determined value of -406×10^{-6} cgs units for $HL\text{-}Et\cdot 0.5H_2O$ with Pascal's constants for the other atoms.[16] A temperature-independent paramagnetism term, TIP, of $+30 \times 10^{-6}$ cgs units/copper atom was included in all calculations because this improved the linearity of the Curie plots at high temperatures in the two cases, $[Cu_2(HL\text{-}Et)(H_2O)_4][ClO_4]_4\cdot H_2O$ and $[Cu_2(L\text{-}Et)(OAc)][ClO_4]_2$, where such linearity is expected. TIP estimates of $(30\text{–}60) \times 10^{-6}$ cgs units are typical for copper(II).[17] All interacting systems were treated in terms of the isotropic $S = {}^1/_2$, $S = {}^1/_2$ spin interaction Hamilton in its $-2J$ form and theoretical molar susceptibilities, χ_M, were calculated from the expression

$$\chi_M = \left(\frac{2N^2\beta^2g^2}{3kT}\right)\left(\frac{1}{1 + [\exp(-2J/k'T)]/3}\right) + \chi_0 + \text{TIP}$$

where symbols have their usual meaning.[18]

Data for the perchlorate complex $[Cu_2(HL\text{-}Et)(H_2O)_4][ClO_4]_4\cdot H_2O$ are displayed graphically as a Curie plot in Figure 1. A combined value of -522×10^{-6} cgs units was used for χ_0 and TIP. The linear data set (●) was obtained from a vacuum-dried sample that was handled in a drybox. The curved set of data (■) was obtained from a sample handled in air. A linear regression analysis on the former data set leads to the solid line in Figure 1. The intercept (Weiss constant) is −2.8 K.

(16) (a) Mulay, L. N. In "Theory and Applications of Molecular Paramagnetism"; Boudreaux, E. A., Mulay, L. N., Ed.; Wiley-Interscience: New York, 1976. (b) O'Conner, C. J. *Prog. Inorg. Chem.* **1982**, *29*, 203–283.

(17) Hellwege, K.-H., Ed. "Landolt-Bornstein New Series"; Springer Verlag: Berlin, 1966 and supplements to 1972.

(18) Drago, R. S. In "Physical Methods in Chemistry"; W. B. Saunders: Philadelphia, 1977; Chapter 11.

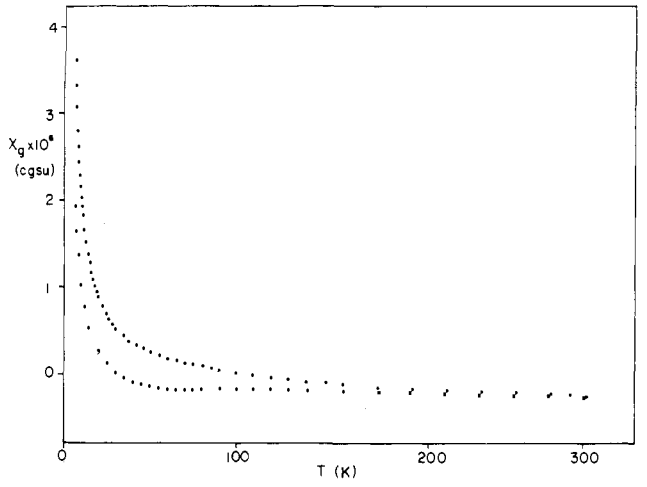

Figure 4. Raw χ_g data for two different preparations of $[Cu_2(L\text{-}Et)(N_3)][BF_4]_2$.

Data on the acetate complex $[Cu_2(L\text{-}Et)(OAc)][ClO_4]_2$ are displayed as a Curie plot in Figure 2. χ_0 + TIP was -449×10^{-6} cgs units. The positive intercept at $\Theta = 8.87$ K from extrapolation of the linear portion of the data (70–300 K) is indicative of a weak ferromagnet. From the approximation $\Theta = J/2K$ that is valid for small and positive values of J, we calculate $J \simeq +12$ cm^{-1}. A more detailed treatment was not attempted because exchange anisotropy as well as intermolecular effects and impurity effects are expected to significantly complicate any interpretation of the low temperature data.

Data for the nitrite complex $[Cu_2(L\text{-}Et)(NO_2)][ClO_4]_2 \cdot H_2O$ are displayed in Figure 3. When the raw data were plotted as gram susceptibilities χ_g vs. temperature, a maximum near 240 K indicated a moderately strong antiferromagnetic exchange. A steep rise in χ_g at very low temperatures suggested the presence of a small amount of a paramagnetic impurity. Consequently, data were corrected for 4.7% of a paramagnetic impurity, assuming it to be $[Cu_2(L\text{-}Et)(H_2O)_4][ClO_4]_4 \cdot H_2O$, a likely contaminant from the synthetic method. A residual curvature of the low-temperature data having a peak at about 40 K was removed by further subtraction of 3.75% of an antiferromagnetic impurity with $J = -18$ cm^{-1} and g = 2.1. These percentages were derived by trial and error with three variables (two percentages and J) using a series of computer-generated data points. The criterion of best fit was approximate constancy of the corrected χ_g values between 6 and 40 K having magnitudes typical of TIP. The corrected χ_M data are displayed in Figure 3. The solid line is a theoretical fit using $g = 2.08$ and $J = -139$ cm^{-1}.

χ_g data for two representative preparations of the azide complex $[Cu_2(L\text{-}Et)(N_3)][BF_4]_2$ are displayed in Figure 4. As in the case of the nitrite complex, a steep rise in χ_g at low temperatures for both samples was indicative of small amounts (1–4%) of paramagnetic impurities. These impurities are not Curie–Weiss law behaved. Further, the two-impurity correction model used above on the nitrite complex was unsuccessful in rendering either data set satisfactorily linear. However, regardless of the interpretation of the nature of these impurities, which can amount to only a few percent, the value of $\chi_g = -2.607 \times 10^{-7}$ cgs units at 300 K in the purest sample indicates that the azide complex is diamagnetic.

Data were collected on the pyrazolate complex $[Cu(L\text{-}Et)(pyl)][ClO_4] \cdot H_2O$ but while they were qualitatively recognizable as arising from a weak antiferromagnet the presence of paramagnetic impurities made a quantitative treatment unreliable.

X-ray Structure Determinations

Data were collected at room temperature on crystals of $[Cu_2(L\text{-}Et)(OAc)][ClO_4]_2$ and $[Cu_2(L\text{-}Et)(N_3)][BF_4]_2$ by using a Syntex $P2_1$ diffractometer with Mo Kα radiation up to a 2θ(max) of 45°. Both structures were solved by Patterson and difference Fourier techniques; the crystallographic data are summarized in Table II. The acetate structure was refined isotropically except for the copper and perchlorate atoms that were treated anisotropically. The azide structure was refined anisotropically except for C14 which was severely disordered. Both structures showed disorder in the *N*-ethyl groups and in the anions which reduces their precision. However, since the important features of the copper coordination spheres were well-defined, no attempt was made to resolve the disorder or locate the hydrogen atoms. Interatomic distances between each cation and its anions were all >3.25 Å.

Selected distances and angles in the two structures are given in Table III. The numbering schemes adopted for each complex cation are shown in diagrams I and II in the supplementary material. The azide complex has a crystallographic C_2 axis through C3, O2, and N7. A full listing of bond distances (Tables A and B) and angles (Tables C and D) for the acetate and azide structures, respectively, is included in the supplementary material. Final atomic coordinates of the acetate structure are listed along with their anisotropic and isotropic thermal parameters in Table

Table II. Crystallographic Data

	$[Cu_2(L\text{-}Et)(OAc)][ClO_4]_2$	$[Cu_2(L\text{-}Et)(N_3)][BF_4]_2$
space group	$P2_1/n$, monoclinic	$C2/m$, monoclinic
a, Å	14.190 (3)	19.082 (3)
b, Å	22.707 (4)	23.896 (3)
c, Å	15.883 (4)	13.230 (2)
β, deg	97.20 (2)	116.21 (1)
Z	4	4
V, Å^3	5077 (2)	5412 (1)
reflctns measd	3808 independent reflctns ($I > 3\sigma(I)$) in the range $2\theta = 3.5$–45°	1631 independent reflctns ($I > 2\sigma(I)$) in the range $2\theta = 3.5$–45°
$R(F)$	9.6	9.5
$R(wF)$	10.7	7.9

Table III. selected bond distances (Å) and angles (deg)

$[Cu_2(L\text{-}Et)(OAc)][ClO_4]_2$

Bond Distances

Cu1–Cu2	3.459 (2)		
Cu1–O2	1.89 (1)	Cu2–O2	1.92 (1)
Cu1–N1	2.13 (1)	Cu2–N6	2.08 (1)
Cu1–N2	2.03 (1)	Cu2–N7	2.06 (1)
Cu1–N4	2.03 (1)	Cu2–N9	2.05 (1)
Cu1–O1	1.93 (1)	Cu2–O3	1.91 (1)
C2–O1	1.22 (2)	C2–O3	1.23 (2)

Bond Angles

Cu1–O2–Cu2	130.6 (5)		
O2–Cu1–N1	84.2 (4)	O2–Cu2–N6	84.2 (4)
O2–Cu1–N2	122.7 (4)	O2–Cu2–N7	119.4 (4)
O2–Cu1–N4	128.4 (4)	O2–Cu2–N9	121.6 (4)
N2–Cu1–N1	81.2 (4)	N7–Cu2–N6	81.7 (4)
N2–Cu1–N4	103.3 (4)	N7–Cu2–N9	113.5 (4)
N1–Cu1–N4	80.9 (4)	N6–Cu2–N9	80.5 (4)
O2–Cu1–O1	95.2 (4)	O2–Cu2–O3	95.7 (4)
N2–Cu1–O1	96.2 (4)	N7–Cu2–O3	98.3 (4)
N1–Cu1–O1	176.4 (4)	N6–Cu2–O3	179.8 (4)
N4–Cu1–O1	102.2 (4)	N9–Cu2–O3	99.7 (4)
Cu1–O1–C2	133.7 (9)	Cu2–O3–C2	133.1 (9)
O1–C2–O3	129 (1)		

$[Cu_2(L\text{-}Et)N_3][BF_4]_2$

Bond Distances

Cu–Cu′	3.615 (3)	Cu–N4	2.11 (1)
Cu–O2	1.944 (8)	Cu–N6	2.04 (1)
Cu–N1	2.06 (1)	N6–N7	1.15 (2)
Cu–N2	2.00 (1)		

Bond Angles

Cu–O2–Cu′	136.9 (6)	O2–Cu–N6	92.3 (5)
O2–Cu–N1	85.9 (5)	N2–Cu–N6	98.8 (5)
O2–Cu–N2	143.8 (4)	N1–Cu–N6	177.8 (5)
O2–Cu–N4	114.2 (4)	N4–Cu–N6	97.1 (5)
N2–Cu–N1	83.4 (5)	N6–N7–N6′	175 (2)
N2–Cu–N4	98.6 (5)	Cu–N6–N7	106 (1)
N1–Cu–N4	82.6 (5)		

E and those of the azide structure in Table F, both in the supplementary material.

Discussion

Synthesis. In general, dimeric copper(II) complexes are readily prepared by self-assembly from monomeric components. But to achieve the degree of ligation control necessary for optimum modelling of the hemocyanin-active site, we felt that a specifically designed binucleating[19] ligand would be required. The design of HL-Et

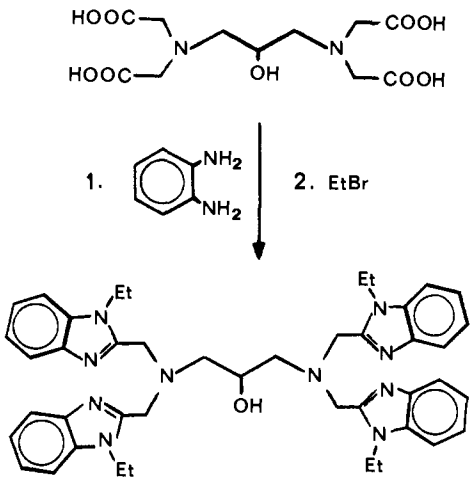

has several useful features. The bond connectivity about the central hydroxy group is well suited to securing two copper atoms in close proximity with or without an alkoxide bridge. There is a balance of symmetry and flexibility to the "arms" of the ligand that leads to readily crystallizable materials having workable solubility. The choice of benzmidazole moieties is an extension of our earlier work which showed the wide scope of the 1,2-diaminobenzene/carboxylic acid condensation reaction for producing new chelating ligands.[7,20] The ligands prepared by Thompson,[21] Reedijk,[6] and Kida[11b] are notable in this regard. Related ligands based on appended pyridine[22,23] and pyrazole[5,24] are also proving to be useful in copper dimer formation. Apart from their ease of synthesis, benzimidazole moieties are desirable for their steric bulk, their chemical inertness (greater than that of imidazoles), and the ready variation of substituents by N-alkylation or ring substitution. They are, of course, good models for histidine residues in proteins and are excellent ligands for both copper(I) and copper(II). The specific derivative HL-Et used in the present work was chosen for its convenient handling properties.

Treatment of HL-Et with 2 equiv of copper(II) perchlorate or tetrafluoroborate results in the formation of complexes of analytical composition $Cu_2(HL\text{-}Et)(H_2O)_5(Y)_4$ ($Y^- = ClO_4^-$ or BF_4^-). The binucleating capacity of the ligand is expressed in the dicopper stoichiometry. The presence of four counterions suggests that the 2-hydroxy group of the binucleating ligand is not deprotonated and is therefore probably not involved in any metal–ligand bonding. Related complexes behave similarly.[25] Strict Curie–Weiss paramagnet behavior down to 6 K of the green perchlorate complex (Figure 1 (●)) also suggests that bridging ligands are not present. However, a broad essentially isotropic EPR signal (g = 2.25) for both the solid and a frozen acetonitrile solution at 16 K indicates that dipolar interactions are present and the copper atoms are probably >4 Å apart. The presence of 1 equiv of a strong base (1,8-bis(dimethylamino)naphthalene) in the synthesis does not appear to lead to deprotonation of the 2-hydroxy group and formation of a single alkoxy bridge. This is surprising in view of the recent reports of formation of single hydroxy-bridged copper(II) dimers[26-29] and a single alkoxy-bridged copper(II) dimer,[30] but space-filling models suggest that steric crowding of the complementary ligands (H_2O or ClO_4^-) might destabilize such a species. Likewise, formation of the more familar dibridged dihydroxy structure[13] is apparently thwarted by intramolecular steric effects and/or constraints from the five-membered chelate rings of HL-Et. Only with added exogenous di- or triatom bridging ligands, as discussed below, does an alkoxide bridge form between the copper(II) atoms.

One idiosyncrasy of the aquo complex is worth brief mention. Upon cooling an undesiccated sample of the green perchlorate complex to dry ice temperature, there is a reversible color change to bright blue. And a Curie plot (Figure 1 (■) of a sample loaded into the susceptometer in air shows two distinct regions of near linearity, one at high temperatures and one at low temperatures, having different slopes (Figure 1). The high-temperature data have a similar slope to the dried material (●). It is apparent that some structural change at copper accompanies a lattice hydration reaction. It is conceptually related to the phase change observed in another copper(II) complex.[31]

If the metalation reaction of HL-Et is followed by the addition of potentially bridging anions X^- (OAc^-, $HCOO^-$, NO_2^-, N_3^-, pyrazolate), spontaneous deprotonation of the ligand occurs to give a series of alkoxide/X^- dibridged complexes:

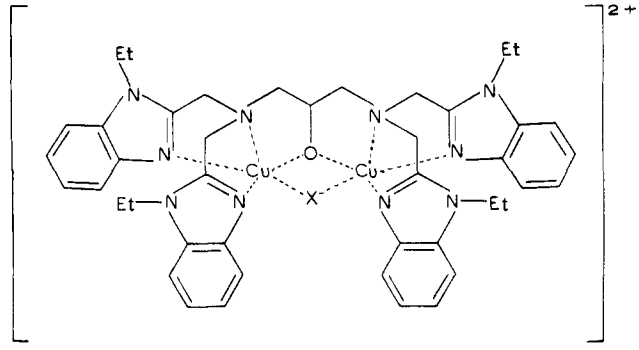

These complexes are the main subject of this paper because of their interesting structural and magnetic properties.

Magnetic Studies. Simply varying X^- in the series of complexes $[Cu_2(L\text{-}Et)X][ClO_4]_2$ leads to quite dramatic changes in the copper–copper magnetic interactions. This was immediately evident from the room-temperature magnetic moments that range from values typical of noninteracting or weakly interacting copper(II) atoms (1.83–1.90 μ_B) through to zero in the diamagnetic azide (Table I). Workup of variable-temperature magnetic susceptibility data for selected complexes reveals that the acetate complex is a weak *ferro*magnet with $J \simeq +12$ cm^{-1}, the pyrazolate is a weak antiferromagnet, the nitrite is a moderately strong antiferromagnet with $J = -139$ cm^{-1}, and the azide is a very strong antiferromagnet. Indeed, the lack of any tendency toward upward curvature of the high-temperature χ_g data points for the azide complex (Figure 4) indicates that diamagnetism is complete, within experimental error. Thus, the error in the highest temperature point, conservatively estimated to be $<10^{-9}$ cgs units, sets an upper

(19) Fenton, D. E. In "Advances in Inorganic and Bioinorganic Mechanisms"; Sykes, A. G., Ed.; Academic Press: London, 1983; Vol. II.
(20) Dagdigian, J. V.; Reed, C. A. *Inorg. Chem.* **1979**, *18*, 2623–2626.
(21) (a) Thompson, L. K.; Ramaswamy, B. S.; Seymour, E. A. *Can. J. Chem.* **1977**, *55*, 878–888. (b) Addison, A. W.; Hendriks, H. M. J.; Reedijk, J.; Thompson, L. K. *Inorg. Chem.* **1981**, *20*, 103–110.
(22) Karlin, K. D.; Gultneh, Y.; Hutchinson, J. P.; Zubieta, J. *J. Am. Chem. Soc.* **1982**, *104*, 5240–5242.
(23) Karlin, K. D.; Hayes, J. C.; Hutchinson, J. P.; Zubieta, J. *J. Chem. Soc., Chem. Commun.* **1983**, 376–378.
(24) Sorrell, T. N.; Malachowski, M. R.; Jameson, D. L. *Inorg. Chem.* **1982**, *21*, 3250–3252.
(25) Sakurai, T.; Kaji, H.; Nakahara, A. *Inorg. Chim. Acta* **1982**, *67*, 1–5.
(26) Haddad, M. S.; Wilson, W. R.; Hodgson, D. J.; Henrickson, D. N. *J. Am. Chem. Soc.* **1981**, *103*, 384–391.
(27) Burk, P. L.; Osborn, J. A.; Youinou, M.-T. *J. Am. Chem. Soc.* **1981**, *103*, 1273–1274.
(28) Coughlin, P. K.; Lippard, S. J. *J. Am. Chem. Soc.* **1981**, *103*, 3228–3229.
(29) Drew, M. G. B.; Nelson, J.; Esho, F.; McKee, V.; Nelson, S. M. *J. Chem. Soc., Dalton Trans.* **1982**, 1837–1843.
(30) McKee, V.; Smith, J. *J. Chem. Soc., Chem. Commun.* **1983**, 1465–1467.
(31) Wood, J. S.; de Boer, E.; Keijzers, C. P. *Inorg. Chem.* **1979**, *18*, 904–906.

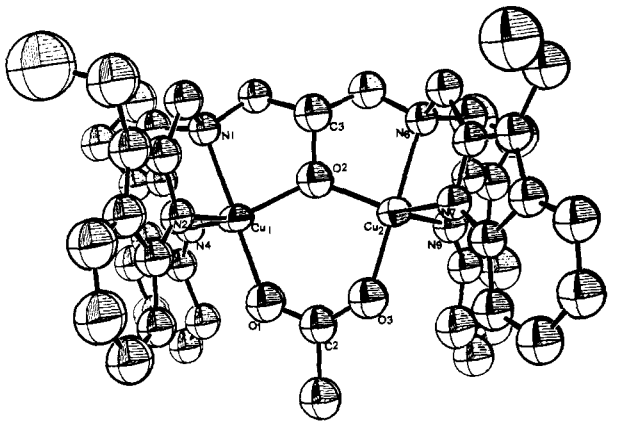

Figure 5. Perspective view (ORTEP, 50%) of the acetate complex $[Cu_2(L\text{-}Et)(OAc)]^{2+}$.

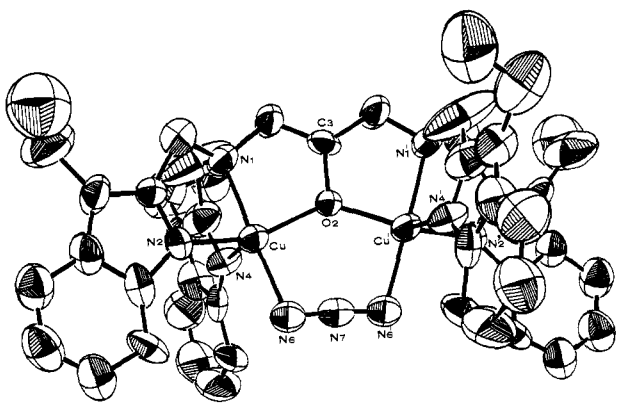

Figure 6. Perspective view (ORTEP, 50%) of the azide complex $[Cu_2(L\text{-}Et)(N_3)]^{2+}$.

limit for any developing paramagnetism in the azide complex arising from uncoupling of the spins. This in turn places a lower limit on the magnitude of the exchange coupling constant such that $|-J| > 550\ cm^{-1}$.

Magnetostructural Correlations. Magnetic interactions in binuclear species are inextricably related to structure. In order to understand the widely varying magnetic moments of the series of dimers $[Cu_2(L\text{-}Et)X]^{2+}$, particularly the diamagnetic azide complex ($X^- = N_3^-$), it was necessary to have definitive structural information. The weakly ferromagnetic acetate complex ($X^- = OAc^-$) and the completely antiferromagnetically coupled azide complex were chosen because both formed single crystals of adequate quality for X-ray analysis and they represent extremes of magnetic behavior.

Perspective views of the acetate and azide complexes are shown in Figures 5 and 6, respectively. Selected bond lengths and bond angles are listed in Table III. Although the two structures are broadly similar, there are significant differences in the detailed coordination geometries, as illustrated in Figure 7. The stereochemistry about Cu2 in the acetate complex closely approximates a trigonal bipyramid. The alkoxy bridge (O2) and the benzimidazoles (N7 and N9) make up the equatorial plane with bond angles that deviate from ideality by only 6.5°. The two Cu2–N(benzimidazole) bond distances are identical within experimental error (2.06 (1), 2.05 (1) Å). The stereochemistry about Cu1 is similar, but the bond angles are somewhat more distorted from ideality. By contrast, the stereochemistry about copper in the azide structure more closely approximates a tetragonal pyramid than a trigonal bipyramid. The angular deviations from ideality are large (see Figure 7), but significantly, the two Cu–N(benzimidazole) bond distances differ by greater than 0.1 Å (Cu–N2 = 2.00 (1) Å; Cu–N4 = 2.11 (1) Å). Apical bond distances typically exceed basal ones in tetragonal-pyramidal copper(II) complexes where valid comparisons can be made. For example, with imidazole coordination, basal distances lie in the range 1.913

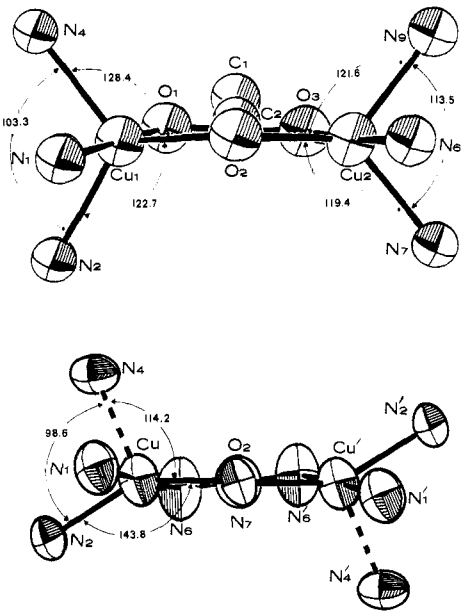

Figure 7. Comparison of the inner coordination sphere stereochemistries of $[Cu_2(L\text{-}Et)(OAc)]^{2+}$ and $[Cu_2(L\text{-}Et)(N_3)]^{2+}$.

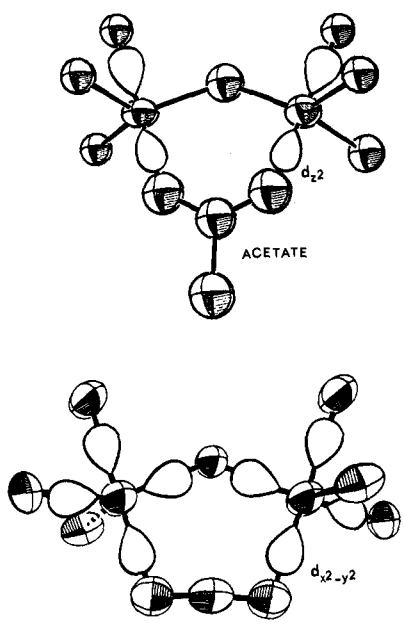

Figure 8. Comparison of the magnetic orbital orientations in the $(d_{z^2})^1$ acetate and the $(d_{x^2-y^2})^1$ azide.

(7)–2.049 (2) Å while an apical interaction has been observed at 2.141 (1).[32] In the azide structure, Cu–N2 has therefore been designated as basal along with the other ligating atoms: N1(amine), O2(alkoxide), and N6(azide). The longer bond to benzimidazole, Cu–N4, is designated as apical and is distinguished in Figure 7 by the dashed line.

We believe that the different coordination geometries of the acetate and the azide complexes offer the most logical explanation for their different magnetic behavior. The argument rests on the notion that a strong magnetic interaction requires both good σ orientation of the magnetic orbitals and good superexchange properties of the bridging atom(s).[33-35] Neither condition is very

(32) Morehouse, S. M.; Polychronopoulou, A.; Williams, G. J. B. *Inorg. Chem.* **1980**, *19*, 3558–3561.
(33) Felthouse, T. R.; Laskowski, E. J.; Hendrikson, D. N. *Inorg. Chem.* **1977**, *16*, 1077–1089.
(34) Hay, J. P.; Thibeault, J. C.; Hoffman, R. *J. Am. Chem. Soc.* **1975**, *97*, 4884–4899.

well satisfied in the acetate complex. The trigonal-bipyramidal stereochemistry dictates a $(d_{z^2})^1$ ground state and thus the major lobes of the magnetic orbital will be axially directed toward a single bridging ligand, the acetate (see Figure 8). By contrast, both conditions are optimized in the azide complex. Its tetragonality can safely be assumed to dictate a $(d_{x^2-y^2})^1$ ground state that orients the magnetic orbital lobes toward both bridging ligands, the alkoxide and the azide. Of the three bridging ligands found in these two complexes, alkoxide is probably the best mediator of superexchange. With the large Cu–O–Cu angles in the present complexes (near 135°) a strong antiferromagnetic superexchange can be expected by analogy to the nearly diamagnetic μ-monohydroxy dimers having similar Cu–O–Cu angles.[26-29] But only in the azide complex is the directionality of the magnetic orbitals appropriate for taking advantage of magnetic exchange via the alkoxide O atom. There is no evidence that a single acetate group can function as a strong mediator of magnetic exchange. The well-known moderately coupled copper(II) acetates[36] usually have four acetate bridges acting in concert. 1,3-Bridging azide is frequently implicated in magnetic exchange pathways with varied magnitude and structure.[29,37] It is difficult to assess its precise role in the present complex other than to conclude that it may substantially augment the antiferromagnetic exchange provided by the alkoxide.

The Bridging Azide Structure. Most of the structural features of the present complexes are typical of five-coordinate copper(II). However, the particular geometry of the 1,3-azide bridge has not been observed before. Normally, a 1,3-azide-bridging mode forces the metal atoms about 6 Å apart.[37] The shortest Cu···Cu separation reported in a 1,3-azido-bridged species is 4.956 (2) Å.[38] In the present complex it is 3.615 (3) Å. This particular 1,3-bridging mode presumably occurs to maintain the complementary alkoxy bridge and to avoid the likely steric congestion of the alternative possibility, a 1,1-bridging mode. As a consequence of the alkoxide bridge the Cu–N–N angles are abnormally acute (106 (1)°). The strain suggested by this less than optimal hybridization may be responsible for the C_2 twist of the azide with respect to the copper–copper vector (~7°) and the slight bending of the azide (N–N–N = 175 (2)°).

Implications for Hemocyanin. The structural features of copper(II) derivatives of hemocyanin are well replicated by the azide complex $[Cu_2(L\text{-}Et)(N_3)]^{2+}$. The requisite minimum of two imidazole ligands per copper, a Cu···Cu separation of ~3.6 Å, and the diamagnetism are found for the first time in a single compound. The additional features of approximate tetragonal stereochemistry, overall five-coordination, an alkoxide bridge, and an azide bridge all lend credence to the structural picture of hemocyanin proposed in Scheme I. In particular, tetragonality of the copper(II) coordination sphere appears to be very important for proper orientation of the magnetic orbitals to achieve diamagnetism. It is clear that the departure from ideal tetragonality can be quite great as long as the bridging ligands are part of the basal "plane". The spontaneous formation of an alkoxide bridge endorses the idea of an endogenous protein bridging ligand and demonstrates that serine or threonine is qualified for this role. The particular geometry of the azide in $[Cu_2(L\text{-}Et)(N_3)]^{2+}$ shows that a 1,3-bridging mode can be accommodated within a 3.6-Å Cu···Cu separation when supported by another bridging ligand. A similar arrangement seems likely in metHc(N_3) since there is considerable congruence of spectroscopic properties. Acetonitrile solutions of the azide complex show a strong UV maximum at 364 nm (414 nm sh) (ϵ 2340 M^{-1} cm^{-1}) that is not present in the acetate complex. A vis maximum is present at 695 nm (ϵ 195). By comparison to bands of very similar energy in metHc(N_3) (*Busycon canaliculatum*) at 360 (ϵ ~1500) and 710 nm (ϵ ~200),[39] they are assigned to azide LMCT and d–d, respectively. The asymmetric azide stretching frequency in the IR spectrum of the complex appears at 2020 (s) cm^{-1} in Nujol or KBr and 2037 (s) cm^{-2} in CH_3CN. In metHc(N_3) the corresponding band is at 2042 cm^{-1}.[40] The compatibility of structure A with metHc(N_3) is very

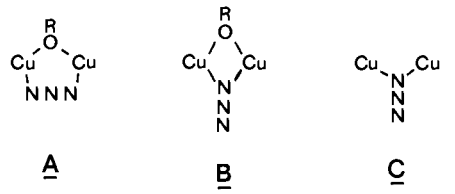

A B C

attractive, but the 1,1-bridging modes B and C should be considered as possible alternatives. However, the 3.1-Å Cu···Cu separations of 1,1-azido-*dibridged* species[41] are incompatible with the 3.66-Å Cu···Cu separation in metHc(N_3), making structure B very unlikely. The possibility that metHc may be simply a monobridged hydroxy species with no endogenous bridging ligand from the protein[27,28] leads to consideration of structure C for metHc(N_3). Triangulation calculations using reasonable Cu–N bond lengths of 2.1 ± 0.1 Å and Cu···Cu separations of 3.6 ± 0.1 Å lead to not unreasonable Cu–N–Cu bridging angles of 120–135°. A potential model for C has been reported,[29] but it shows very little magnetic coupling. Since the magnitude of J will be very dependent upon the bridgehead Cu–N–Cu angle, one should be cautious about eliminating C solely on magnetic grounds. However, exogenous monobridged formulations for the closely related metHc(OAc) and HcO_2 are unlikely on both geometric and magnetic grounds and we do not believe structure C is likely in metHc(N_3). Moreover, new titration evidence for dibridged rather than monobridged metHc(N_3) has recently been presented.[42]

In conclusion, the essential features of the active site structural chemistry of methemocyanin can be reproduced in an appropriately chosen model compound. The spectroscopically effective structure[1e] is seen to be entirely consistent with the intrinsic dinuclear coordination chemistry of copper(II), and the model compound $[Cu_2(L\text{-}Et)(N_3)]^{2+}$ provides an excellent reference point for further structural refinement and reactivity studies. In the absence of a high-resolution X-ray crystallographic structure for hemocyanin[43] the model compound approach is turning out to be a useful probe of its coordination chemistry.[44]

Acknowledgment. The assistance of Professor Robert Bau in solving the crystal structures, Drs. Frank DiSalvo and Joseph Waszczak (Bell Labs) in early magnetic studies, and useful discussions with Dr. Jean-Marc Latour (CENG) are greatefully acknowledged. This work was supported by the NIH (Grant AM 30801) and, in part, by the NSF (Grant CHE 8026812 and Squid Instrumentation Grant CHE 8211349).

Registry No. HL-Et, 79724-80-4; $[Cu_2(HL\text{-}Et)(H_2O)_4][ClO_4]_4$, 90991-14-3; $[Cu_2(HL\text{-}Et)(H_2O)_4][BF_4]_4$, 90991-15-4; $[Cu_2(L\text{-}Et)(OAc)][ClO_4]_2$, 79736-52-0; $[Cu_2(L\text{-}Et)(N_3)][ClO_4]_2$, 90991-17-6;

(35) Girerd, J. J.; Kahn, O.; Verdaguer, M. *Inorg. Chem.* **1980**, *19*, 274–276.
(36) Doedens, R. J. *Prog. Inorg. Chem.* **1976**, *21*, 209–231.
(37) (a) Felthouse, T. R.; Hendrikson, D. N. *Inorg. Chem.* **1978**, *17*, 444–456. (b) Barraclough, C. G.; Brooks, R. W.; Martin, R. L. *Aust. J. Chem.* **1974**, *27*, 1843–1850. (c) Comarmond, J.; Plumere, P.; Lehn, J.-M.; Agnus, Y.; Louis, R.; Weiss, R.; Kahn, O.; Morgenstern-Badarau, I. *J. Am. Chem. Soc.* **1982**, *104*, 6330–6340. (d) Kahn, O.; Sikarav, S.; Gouteron, J.; Jeannin, S.; Jeannin, Y. *Inorg. Chem.* **1983**, *22*, 2877–2883 and references within these papers.
(38) Zido, R. F.; Gaughan, A. P.; Dori, Z.; Pierpont, C. G.; Eisenberg, R. *Inorg. Chem.* **1971**, *10*, 1289–1296.
(39) Himmelwright, R. S.; Eickman, N. C.; LuBien, C. D.; Solomon, E. I. *J. Am. Chem. Soc.* **1980**, *102*, 5378–5388.
(40) Solomon, E. I., personal communication.
(41) Karlin, K. D.; Hayes, J. C.; Hutchinson, J. P.; Zubieta, J. *J. Chem. Soc., Chem. Commun.* **1983**, 376–378.
(42) Wilcox, D. E.; Long J. R.; Solomon, E. I. *J. Am. Chem. Soc.* **1984**, *106*, 2186–2194.
(43) van Schaick, E. J. M.; Schutter, W. G.; Gaykerna, W. P. J.; Schepman, A. M. H.; Hol, W. G. J. *J. Mol. Biol.* **1982**, *158*, 457–485. Gaykema, W. P. J.; van Schaick, E. J. M.; Schutter, W. G. J.; Hol, W. G. J. *Chem. Scr.* **1983**, *21*, 19–23.
(44) For related model compound approaches see: Nelson, S. M.; Esho, F.; Lavery, A.; Drew, M. G. B. *J. Am. Chem. Soc.* **1983**, *105*, 5693–5995. Sorrell, T. N.; Jameson, D. L.; O'Conner, C. J. *Inorg. Chem.* **1984**, *23*, 190–195. Agnus, Y.; Louis, R.; Gisselbrecht, J.-P.; Weiss, R. *J. Am. Chem. Soc.* **1984**, *106*, 93–102 and references within these papers.

$[Cu_2(L\text{-}Et)(N_3)][BF_4]_2$, 79736-45-1; $[Cu_2(L\text{-}Et)(pyl)][ClO_4]_2$, 79736-48-4; $[Cu_2(L\text{-}Et)(NO_2)][ClO_4]_2$, 79736-50-8; $[Cu_2(L\text{-}Et)(HCOO)][ClO_4]_2$, 90991-19-8; 1,2-diaminobenzene, 95-54-5; 2-hydroxy-1,3-diaminopropanetetraacetic acid, 3148-72-9.

Supplementary Material Available: Atom numbering schemes (diagrams I and II) and tables of bond lengths (Tables A and B), bond angles (Tables C and D), and final atomic coordinates and thermal parameters (Tables E and F) for the acetate and azide complexes, respectively (19 pages). Ordering information is given on any current masthead page.

Thermal and Light-Induced Reduction of $Ru(bpy)_3^{3+}$ in Aqueous Solution

Pushpito K. Ghosh, Bruce S. Brunschwig, Mei Chou, Carol Creutz,* and Norman Sutin*

Contribution from the Department of Chemistry, Brookhaven National Laboratory, Upton, New York 11973. *Received August 22, 1983*

Abstract: The spontaneous reduction of $Ru(bpy)_3^{3+}$ to $Ru(bpy)_3^{2+}$ in aqueous solutions yields only trace O_2 and is accompanied by degradation of ~10% of the tris(bipyridine) complex. Carbon dioxide (5–6 mol of CO_2 per 100 mol of $Ru(bpy)_3^{3+}$ taken) is produced over the entire pH range, 0 to 12. In addition, modified $Ru(bpy)_3^{2+}$-like complexes whose yields (0.2–5.9 mol of Ru per 100 mol of $Ru(bpy)_3^{3+}$ taken) are a function of pH have been identified as products by high-performance liquid chromatographic analysis of the product solutions. The latter have been partially characterized by electrochemical and spectroscopic techniques and are not formed when sufficient Co^{2+}_{aq} (which catalyzes O_2 formation) is added to the reaction mixture. At pH 7, near stoichiometric O_2 formation is found for $(0.01\text{–}1.0) \times 10^{-3}$ M initial $Ru(bpy)_3^{3+}$ when the Co(II) catalyst concentration is $\simeq 0.1$ $[Ru(III)]_0$ and added [Ru(II)] is ≤ 10 $[Ru(III)]_0$. Kinetic studies as a function of pH, [Co(II)], $Ru(bpy)_3^{3+}$, and $Ru(bpy)_3^{2+}$ give the rate law $-d[Ru(III)]/dt = k[Ru(III)]^2[Co(II)]/[Ru(II)][H^+]^2$ ($k = 5.3 \times 10^{-10}$ M s^{-1} at 25 °C, 0.1 M ionic strength, pH 6.5–7.2) thus implicating a Co(IV) species as a crucial intermediate in O_2 formation. Irradiation of $Ru(bpy)_3^{3+}$ solutions with red light ($\lambda = 660 \pm 30$ nm) accelerates the reduction of $Ru(bpy)_3^{3+}$; the quantum yields for Ru(II) and CO_2 formation are 7×10^{-5} and 2.8×10^{-6} mol/einstein, respectively, in 4 M H_2SO_4 or CF_3SO_3H and 2×10^{-4} and 1.1×10^{-5} mol/einstein, respectively, in 1 M H_2SO_4 or CF_3SO_3H.

The reduction of $Ru(bpy)_3^{3+}$ in aqueous solution is a reaction of considerable current interest[1,2] since eq 1, in which water is oxidized to O_2, forms part of a scheme for water photodecomposition when combined with eq 2. Despite the desirability of

$$Ru(bpy)_3^{3+} + {}^1/_2H_2O \rightarrow Ru(bpy)_3^{2+} + {}^1/_4O_2 + {}^1/_2H^+ \quad (1)$$

$$Ru(bpy)_3^{2+} + H^+ \rightarrow Ru(bpy)_3^{3+} + {}^1/_2H_2 \quad (2)$$

eq 1, O_2 is formed stoichiometrically only in the presence of added catalysts such as Co^{2+}_{aq},[3,4] ruthenium complexes,[5,6] and metal oxide suspensions, and even then O_2 formation is more the exception than the rule.[7,8] Reduction of $Ru(bpy)_3^{3+}$ to $Ru(bpy)_3^{2+}$ occurs in aqueous media without O_2 formation over a wide range of conditions, and the nature of the oxidized products and the mechanism of their formation is of some interest. Similar behavior has been found for the analogous Fe(III) and Os(III) complexes.[9-11] Earlier preliminary studies of the products in the $Ru(bpy)_3^{3+}$ system showed that most (>90%) of the ruthenium-containing product is $Ru(bpy)_3^{2+}$ even when no O_2 is produced.[1] Here we have used high-performance liquid chromatographic techniques[12] to separate the other complexes produced in the reaction and have also identified CO_2 as a product of the decomposition.[13] In addition we have investigated the photoreduction of $Ru(bpy)_3^{3+}$ in acid media and find similar products for both thermal and photochemical paths. Finally, we have studied the Co(II) catalysis of O_2 formation by $Ru(bpy)_3^{3+}$ and, from the rate law in the neighborhood of pH 7, find that Co(IV) is implicated as an intermediate in the catalytic sequence.[4]

Experimental Section

Materials. $[Ru(bpy)_3]Cl_2 \cdot 6H_2O$ (G. F. Smith) was recrystallized twice from water. $[Ru(bpy)_3](ClO_4)_2$ was prepared by adding 4 M $HClO_4$ to an aqueous solution of $[Ru(bpy)_3]Cl_2$. The perchlorate salt was separated by filtration and dissolved in 0.5 M H_2SO_4. A scoop of PbO_2 was added, and the solution was stirred at room temperature and filtered through a fine frit. The perchlorate concentration of the filtrate was adjusted to ~2 M by the dropwise addition of $HClO_4$, and the solution was then cooled in an ice bath. Green crystals of $[Ru(bpy)_3](ClO_4)_3$ rapidly formed and were recrystallized from 4 M $HClO_4$ at 0 °C.

The complex $[Ru(bpy)_2(bpyO)](PF_6)_2$ (bpyO is bipyridine *N*-oxide, prepared via reaction of bpy with H_2O_2 in glacial acetic acid[14a]) was synthesized from $Ru(bpy)_2(dme)_2^{2+}$ (dme = dimethoxyethane)[14b] and bpyO under dry, anaerobic conditions. The chloride salt $[Ru(bpy)_2(bpyO)]Cl_2$ was isolated by treating a solution of the PF_6^- salt in acetone with tetrabutylammonium chloride. The material is extremely photosensitive and its photochemistry is currently under detailed study. IR (cm^{-1}) (chloride salt, KBr pellet): ν_{NO} 1226 (vs), 1240 (s), 1228 (sh); δ_{NO} 839 (vs).[14c]

Puratronic grade $CoSO_4$ was obtained from Johnson Matthey. Peroxide solutions were prepared by dilution of a commercial 30% solution and standardized from the absorbance decreases resulting when known

(1) Creutz, C.; Sutin, N. *Proc. Natl. Acad. Sci. U.S.A.* **1975**, *72*, 2858.
(2) Lehn, J. M.; Sauvage, J. P.; Ziessel, R. *Nouv. J. Chim.* **1979**, *3*, 423.
(3) Shafirovich, V. Ya.; Khannanov, N. K.; Strelets, V. V. *Nouv. J. Chim.* **1980**, *4*, 81.
(4) Brunschwig, B. S.; Chou, M. H.; Creutz, C.; Ghosh, P.; Sutin, N. *J. Am. Chem. Soc.* **1983**, *105*, 4832.
(5) Gersten, S. W.; Samuels, G. J.; Meyer, T. J. *J. Am. Chem. Soc.* **1982**, *104*, 4029.
(6) Goswami, S.; Chrakravarty, A. R.; Chakravorty, A. *J. Chem. Soc., Chem. Commun.* **1982**, 1288.
(7) Lehn, J. M.; Sauvage, J. P.; Ziessel, R. *Nouv. J. Chim.* **1980**, *4*, 355.
(8) Kiwi, J.; Kalyanasundaram, K.; Grätzel, M. *Struct. Bonding (Berlin)* **1982**, *49*, 37.
(9) Nord, G.; Wernberg, O. *J. Chem. Soc., Dalton Trans.* **1972**, 866.
(10) Nord, G.; Wernberg, O. *J. Chem. Soc., Dalton Trans.* **1975**, 845.
(11) Nord, G.; Pedersen, B.; Bjergbakke, E. *J. Am. Chem. Soc.* **1983**, *105*, 1913.
(12) Valenty, S. J.; Behnken, P. E. *Anal. Chem.* **1978**, *50*, 834.
(13) The formation of CO_2 is also reported by: Shafirovich, V. Ya.; Strelets, V. V. *Nouv. J. Chim.* **1982**, *6*, 183. CO_2 is produced in even higher yield in the $Ni(bpy)_3^{3+}$ system (S.-F. Chan, work in progress).
(14) (a) Murase, I. *Nippon Kagaku Zasshi* **1966**, *77*, 682; *Chem. Abstr.* **1958**, *52*, 9100a. (b) Connor, J. A.; Meyer, T. J.; Sullivan, B. P. *Inorg. Chem.* **1979**, *18*, 1388. (c) See: Speca, A. N.; Karayannis, N. M.; Pytlewski, L. L.; Winters, L. J.; Kandasamy, D. *Inorg. Chem.* **1973**, *12*, 1221.

0002-7863/84/1506-4772$01.50/0